Molecular Vision 2006; 12:1306-18 <http://www.molvis.org/molvis/v12/a148/>
Received 26 April 2006 | Accepted 6 October 2006 | Published 27 October 2006

Uptake of cholesterol by the retina occurs primarily via a low density lipoprotein receptor-mediated process

Nomingerel Tserentsoodol,[1] Jorge Sztein,[2] Mercedes Campos,[3] Natalya V. Gordiyenko,[1] Robert N. Fariss,[3] Jung Wha Lee,[1] Steven J. Fliesler,[4] Ignacio R. Rodriguez[1]

[1]Laboratory of Retinal Cell and Molecular Biology, Section on Mechanisms of Retinal Diseases, [2] Veterinary Research and Resources Section, [3]Biological Imaging Core, National Eye Institute, National Institutes of Health, Bethesda, MD, [4]Saint Louis University Eye Institute and Department of Pharmacological and Physiological Science, Saint Louis University School of Medicine, Saint Louis, MO

Purpose: In this study we examined the uptake of circulating lipoproteins into the retina, using a naturally fluorescent cholesterol analog for imaging and deuterated cholesterol for quantification by mass spectroscopy. The purpose of this study was to better understand cholesterol uptake, transport and homeostasis in the retina.
Methods: Human low density lipoprotein (LDL) and high density lipoprotein (HDL) were labeled with the fluorescent cholesterol analog cholesta-5,7,9(11)-trien-3βol (CTL) and deuterated cholesterol (25,26,26,26,27,27,27-[^{2}H]cholesterol, D7Ch). Rats were injected intravenously with CTL-LDL, CTL-HDL and D7Ch-LDL. Fluorescent confocal microscopy was used to image the uptake of CTL and mass spectroscopy was used to quantify D7Ch. Immunohistochemistry and fluorescent confocal microscopy were used to localize apoB (an LDL marker protein) and LDL receptor (LDLR) protein in rat and monkey retinas.
Results: CTL-specific fluorescence was imaged by confocal microscopy in the retinal pigment epithelium (RPE), choriocapillaris and parts of the neural retina within 2 h post-injection and was visualized in the photoreceptor outer segments by 4 h. Replacing LDL with HDL as the CTL carrier gave a less robust and more delayed labeling of retinal layers. Human apolipoprotein B (apoB) was also localized in the rat choriocapillaris and RPE by 4 h post-injection. Human apoB was detected by immunoblot analysis in the rat retina primarily as a about 70 kDa protein, suggesting proteolytic degradation. LDL-mediated uptake of cholesterol was quantified by mass spectroscopy using deuterated cholesterol in place of CTL. In addition, apoB and LDLR were localized in monkey retina by immunohistochemistry.
Conclusions: The retina is capable of rapid uptake of circulating LDL via an LDLR-mediated process primarily occurring in the RPE and also possibly Müller cells. Despite the dominance of HDL over LDL in rat serum, LDL appears to be the preferred carrier for cholesterol transport to and uptake by the retina. The results also suggest that blood-borne LDL represents a significant contributor to the steady-state levels of cholesterol and possibly other lipids in the retina.

Despite nearly three decades of investigation, lipid metabolism and transport in the retina are not fully understood. Although the retina is capable of synthesizing cholesterol and other lipids de novo, this cannot fully account for the steady-state lipid composition of the retina, suggesting that extraretinal sources of lipid contribute, in part, to the retinal lipid composition [1-5]. The relative contribution of de novo (intraretinal) synthesis versus extraretinal uptake to the overall content of lipids in the retina remains unknown. However, several independent lines of evidence indicate that plasma low-density lipoproteins (LDL) are internalized by LDL receptors (LDLRs) and/or scavenger receptors and serve as a significant source of lipids for the retina. Such receptors have been localized to the retinal pigment epithelium (RPE), the cellular interface between the neural retina and the choroidal vasculature, using biochemical and immunohistochemical methods [6,7]. The retina is highly enriched in polyunsaturated fatty acids, especially docosahexaenoic acid (DHA, C22:6ω3), which is supplied via blood-borne LDL [8,9]. More recently, a study using monkeys [10] demonstrated that LDL could deliver ω-3 fatty acids to the RPE, causing induction of acid lipase with concomitant reduction of lipofuscin accumulation. Also, it has been shown that LDL is an efficient vehicle for delivering benzoporphyrin (a lipophilic photodynamic therapy agent) throughout the retina [11,12]. Recently, intravenously injected, rhodamine-labeled LDL in rats was demonstrated to form deposits in Bruch's membrane and to label the RPE [13]. Thus, circulating LDL seems to be a potentially significant source of lipids for the retina, as well as a suitable vehicle for delivering lipid-soluble agents to the retina.

LDL-mediated lipid uptake by the retina raises a number of questions regarding lipid transport and homeostasis. The retina has two blood supplies: the choriocapillaris, which essentially feeds the RPE via fenestrated junctions and is the major, if not sole, source of nutrient supply to the photoreceptors; and the inner retinal vessels, which have tight junctions and are surrounded by Müller cells, the glial cells of the retina [14,15]. Thus, LDL only needs to cross Bruch's membrane

Correspondence to: Ignacio R. Rodriguez, National Eye Institute, NIH, Mechanisms of Retinal Diseases Section, LRCMB, 7 Memorial Drive, MSC0706, Bldg. 7 Rm. 302, Bethesda, MD 20892; Phone: (301) 496-1395; FAX: (301) 402-1883; email: rodriguezi@nei.nih.gov

(the extracellular matrix interface between the choriocapillaris and the basal surface of the RPE) to reach the RPE, while in the neural retina it has to cross the capillary endothelial cells to reach the Müller cells. LDL is a lipoprotein particle synthesized by the liver and contains approximately 20% protein (apoB-100) and 80% lipid, by weight [16]. The lipids are comprised of a mixture of free cholesterol, cholesterol esters (CE), phospholipids (PL) and triglycerides (TG). The uptake of LDL by cells is dependent on cognate receptors, LDLRs [17,18], which recognize apolipoprotein B (apoB) and form a complex with LDL that subsequently enters the cell via endocytosis of clathrin-coated pits. The complexes are then delivered to the endosomes, whereupon LDL is released from the receptor and is subsequently delivered to and degraded by the lysosomes. The brain, which synthesizes most, if not all, of its own cholesterol [19], uses endogenous apolipoprotein E (apoE) to transport cholesterol within the central nervous system [20]. The retina, by contrast, although technically a part of the central nervous system, has the capacity both to synthesize cholesterol de novo and to take up blood-borne lipids [3]. This suggests that the retina also must have an internal lipid transport mechanism to distribute lipids to cells that are not immediately adjacent to the vascular network.

In this study, using two divergent vertebrate species (rats and monkeys), we provide biochemical and correlative immunohistochemical evidence that strongly implicates LDL as the dominant vehicle for delivery of blood-borne cholesterol (and likely other lipids) to the retina and suggests that LDL-borne lipids significantly contribute to the retina's steady-state lipid composition. Immunohistochemical localization of LDLR and apoB in monkey retina is consistent with the biochemical evidence and provides, by inference, the appropriate relevance to lipid uptake by and transport within the human retina.

METHODS

Materials: Cholestatrienol (CTL, cholesta-$\Delta^{5,7,9(11)}$-trien-3β-ol) was synthesized from 7-dehydrocholesterol as previously described [21]. Following multiple recrystallizations, its purity was assessed to be >99% by HPLC and by LC-MS. Deuterated cholesterol (25,26,26,26,27,27,27-[^{2}H]cholesterol; >99% pure, D7Ch) was used as purchased from Cambridge Isotope Laboratories, Inc. (Andover, MA). Sheep anti-human apoB100 (used on rat retina specimens) was purchased from Abcam (Cambridge, MA). Mouse monoclonal anti-human apoB antibody (used on monkey retina specimens) was purchased from BD Biosciences (San Jose, CA). Rabbit anti-human LDLR polyclonal antibody was purchased from Santa Cruz Biotechnology, Inc. (Santa Clara, CA). Donkey anti-sheep 633 Alexa Fluor®-conjugated secondary antibody was purchased from Molecular Probes, Inc. (Eugene, OR). Cy5-conjugated donkey anti-mouse and Cy5-conjugated goat anti-rabbit secondary antibodies were purchased from Jackson ImmunoResearch Laboratories, Inc., (West Grove, PA). HPLC quality solvents were purchased from Fisher Scientific, Inc. (Fair Lawn, NJ). Cholesterol was used as purchased from Steraloids (Newport, RI). Human HDL was purchased from Sigma-Aldrich (St. Louis, MO).

High pressure liquid chromatography and mass spectroscopy: Analyses of cholesterol and deuterated cholesterol were performed using a Waters Corporation (Milford, MA) Model 2695 Separations module high-pressure liquid chromatography instrument equipped with a Model 2996 photodiode array UV detector (PDA) and a Waters/Micromass Q-TOF micro mass spectrometer equipped with an ionSabre® atmospheric pressure chemical ionization probe (APCi). Data collection was performed using MassLynx® version 4.0 in a PC running Windows XP. The HPLC was performed as previously described [22]. The LC flow of 1 ml/min was passed through the PDA detector and then into the Q-TOF. The APCi probe was used in positive mode with the temperature set to 470 °C and the source temperature to 120 °C. The cone gas and the desolvation gas flow were set to 50 and 600 l/h, respectively. The corona was set to 10 μA, the sample cone to 25 V and the extraction cone to 3 V. In the quadrupole the ion energy was set to 2 V and the collision energy to 7 V to prevent further fragmentation of the ions. Cholesterol was detected as a positive ion with an m/z of 369 which reflects its mass (386) minus 17 or a hydroxyl ion (M-OH+). D7Ch was detected as an m/z of 376 reflecting 7 additional masses due to the deuterium substitutions in its side chain.

Cell culture: ARPE19 cells were purchased from American Type Culture Collection (Manassas, VA). The cells were cultured in DMEM/F12 (1:1, by vol.) medium containing 10% fetal bovine serum (Atlanta Biological Inc., Atlanta, GA), 2 mM glutamine, 100 IU/ml penicillin, and 100 μg/ml streptomycin (all from Invitrogen Corp., Carlsbard, CA).

Purification of human low density lipoprotein: Human LDL was purified by as previously described [23]. Serum was collected from normal lipidimic donors and mixed with a solution of NaCl:KBr (1.346 g/ml) to a density of 1.063 g/ml. The adjusted serum was centrifuged at 105,000 xg in a Beckman Ultracentrifuge for 20 h. The LDL was collected as a yellowish band and dialyzed in PBS containing 1 mM EDTA.

Labeling of low density lipoprotein and high density lipoprotein: Cholestatrienol (1 mg) was dissolved in 200 μl of ethanol and added to 10 ml of 1 mg/ml LDL or HDL (total) in PBS containing 5 mM EDTA. The two samples were mixed quickly and allowed to stand at room temperature for 30 min. The sample was then concentrated to 10 mg/ml using an Amicon Ultra centrifugal filter device (50,000 MWCO, Millipore, Billerica, MA) and washed with three volumes of PBS containing 1 mM EDTA. The D7CH-LDL was prepared in the same manner except replacing CTL with D7Ch.

Rat injections with cholestatrienol-low density lipoprotein and tissue preparation: Sprague-Dawley albino male rats (300-350 g) were purchased from Charles River (Charles River, MA). The rats were anesthetized with 40-80 mg of ketamine and 8 mg xylazine per kg of body weight before intravenous injection with LDL. The rats were injected with 0.2 ml of CTL-LDL suspension (10 mg/ml in PBS) via the penile vein, using a 30 gauge needle and a 1-cc tuberculin syringe. The rats were euthanized at 2, 4, 6, 8, 16, 18, and 24 h post injection in an uncharged CO_2 chamber. The eyes were fixed in 4% paraformaldehyde in PBS for 4 h then embedded in 5% agarose type

XI (Sigma-Aldrich). The rats were treated in accordance with the ARVO Statement for the Use of Animals in Ophthalmic and Vision Research.

Immunoflourescence staining and confocal microscopy rat retinal tissue: Vibrotome sections (100 μm) were prepared using a vibrating-blade microtome (Leica Vt 1000s, Microsystems Nussolch GmbH, Nussloch, Germany) equipped with a sapphire knife (Electron Microscopy Sciences, Hatfield, PA). The rat retina sections were blocked in PBS containing normal goat serum (diluted 1:10, by vol.), 0.5% BSA, 0.2% Tween-20 and 0.05% sodium azide for 4 h at 4 °C. The capillary endothelial cells were labeled with *Griffonia simplicifolia* lectin (Isolectin GS-IB_4, AlexaFluor 488 conjugate; Molecular Probes, Eugene, OR). The nuclei were stained with propidium iodide (1 μg/ml). The slides were mounted with Gel/Mount; (Biomeda Corp) and imaged using a Leica SP2 scanning confocal microscope (Leica Microsystems, Exton, PA) equipped with a Leica 40x HCX 1.25 N.A. oil immersion lens. The images were taken at 1024x1024 pixels resolution. To minimize cross-channel bleed through images were collected in sequential scan mode. Cholestatrienol (blue) was visualized by exciting with 351 and 364 nm lasers and collecting emissions between 410-470 nm. Alexa Fluor® 488 (green) was visualized by exciting with the 488 nm laser and collecting emissions between 500-552 nm. Propidium iodide was excited with the 568 nm laser, collecting emissions between 580-650 nm. The sheep anti-human apoB100 was detected using a donkey anti-sheep Alexa Fluor® 633 conjugated secondary antibodies (Molecular Probes, Eugene, OR) which was excited with the 633 nm laser and emissions were collected between 653-750 nm. Magnifications varied, and scale bars are therefore digitally included the pictures.

SDS-polyacrylamide gel electrophoresis (SDS-PAGE) and immunoblotting (western blot) analyses: Protein samples were mixed with NuPAGE® LDS sample buffer and NuPAGE® reducing agent (Invitrogen Corp., Carlsbad, CA) and incubated at 65 °C for 10 min. The samples (20 μg each) were separated in 4-12% NuPAGE Novex Bis-Tris Gels running in 1x NuPAGE® MOPS SDS running buffer at room temperature for 50 min at 200 V. The protein electrophoresis reagents and apparatuses were purchased from Invitrogen/NOVEX (Carlsbad, CA). The gels were transferred onto a PROTRAN®-nitrocellulose membrane (Schleicher and Schuell BioScience Inc., Keene, NH) using a Trans-Blot electrophoresis apparatus (Bio-Rad, Hercules, CA). The transfer was performed in NuPAGE Transfer Buffer and 10% methanol at 30 V, 4 °C overnight. The membrane was equilibrated in 1x Tris-buffered Saline pH 7.4 (TBS) Tween-20 for 15 min, and blocked in 1x TBS, pH 7.4, 5% Carnation nonfat milk and 1% western blocking reagent (Roche Diagnostics Corp., Indianapolis, IN) for 2 h. Incubations with primary antibodies were performed overnight at 4 °C, followed by 1 h of incubation with anti-rabbit, anti-sheep (Pierce Biotechnology, Inc., Rockford, IL) and anti-mouse (Santa Cruz Biotechnologies, Inc., Santa Cruz, CA) IgG peroxidase conjugated secondary antibodies at a dilution of 1:50,000. Blots were developed on X-ray film using SuperSignal West Pico Chemiluminescent Substrate (Pierce, Rockford, IL) after a 10-120 s exposure. The SeeBlue Plus2® Pre-Stained Standard (10 μl) and/or HiMark® pre-stained Standard (10 μl) were used for the estimation of molecular weights on the gels and blots (Invitrogen Corp., Carlsbad, CA).

Monkey retinal tissue: Fresh eye tissue was obtained from rhesus monkeys (*Macacca mulatta*, 2-3 years old) though the courtesy of the Center for Biologics Research and Testing, U.S. Food and Drug Administration (Bethesda, MD). Vibrotome sections were prepared as describe above for rat retina.

Immunohistochemistry of monkey retina: Vibrotome sections (100 μm thickness) were blocked (see description, above) and then incubated with either anti-human apoB mouse monoclonal antibody or rabbit anti-human LDLR primary antibodies at 1:100 dilutions. Cy5 conjugated donkey anti-mouse and Cy5 conjugated goat anti-rabbit secondary antibodies (Jackson ImmunoResearch Laboratories, Inc., West Grove, PA) were used at 1:1000 dilutions for 4 h at room temperature. Alexa Fluor 488-conjugated Isolectin GS-IB_4 (1:500 dilution) was used to stain capillary endothelial cells (see above), while nuclei were counterstained with 4',6'-diamino-2-phenylindole (DAPI; 1 μg/mL in PBS). The slides were mounted (GelMount; Biomeda Corp., Foster City, CA) and kept in the dark until viewing. The Cy5 conjugated secondary antibodies were visualized by exciting with the 633 nm laser beam and collecting emissions between 650-750 nm.

RESULTS

Cholestatrienol-low density lipoprotein uptake by the rat retina: To specifically examine the delivery and uptake of cholesterol by the retina via blood-borne LDL, we modified human LDL to contain cholestatrienol (CTL), a blue-fluorescing cholesterol analog, and injected the fluorescently tagged lipoproteins intravenously into albino rats. CTL is structurally very similar to cholesterol and has been shown to faithfully mimic its membrane properties [21,24,25]. Also, the ultraviolet excitation and blue emission spectra of this compound do not interfere with any of the commonly used green or red fluorophores, making it particularly well suited for double and triple labeling experiments.

Albino Sprague-Dawley rats (around 350 g) were injected with 2 mg of total (protein plus lipid weight) human CTL-LDL and sacrificed at different time intervals. Subsequently, the eyes were fixed, embedded, and vibrotome sections prepared there from were examined by confocal fluorescence microscopy. The results are shown in Figure 1. By 2 h post-injection, CTL-specific fluorescence (blue) was visible in the RPE, choroid, and photoreceptor inner segments (Figure 1A,B). By 4 h, CTL labeling was visible throughout the retina (Figure 1C,D), including the photoreceptor outer segments. Maximum fluorescence in the retina was detected at 6 h post-injection (Figure 1E,F). By 24 h, most of the CTL-LDL had cleared the choriocapillaris and the inner retina, but the photoreceptors and RPE remained labeled. Also, a substantial number of blue-fluorescing punctuate deposits remained visible in the choriocapillaris (Figure 1G,H).

Cholestatrienol-low density lipoprotein uptake by the rat

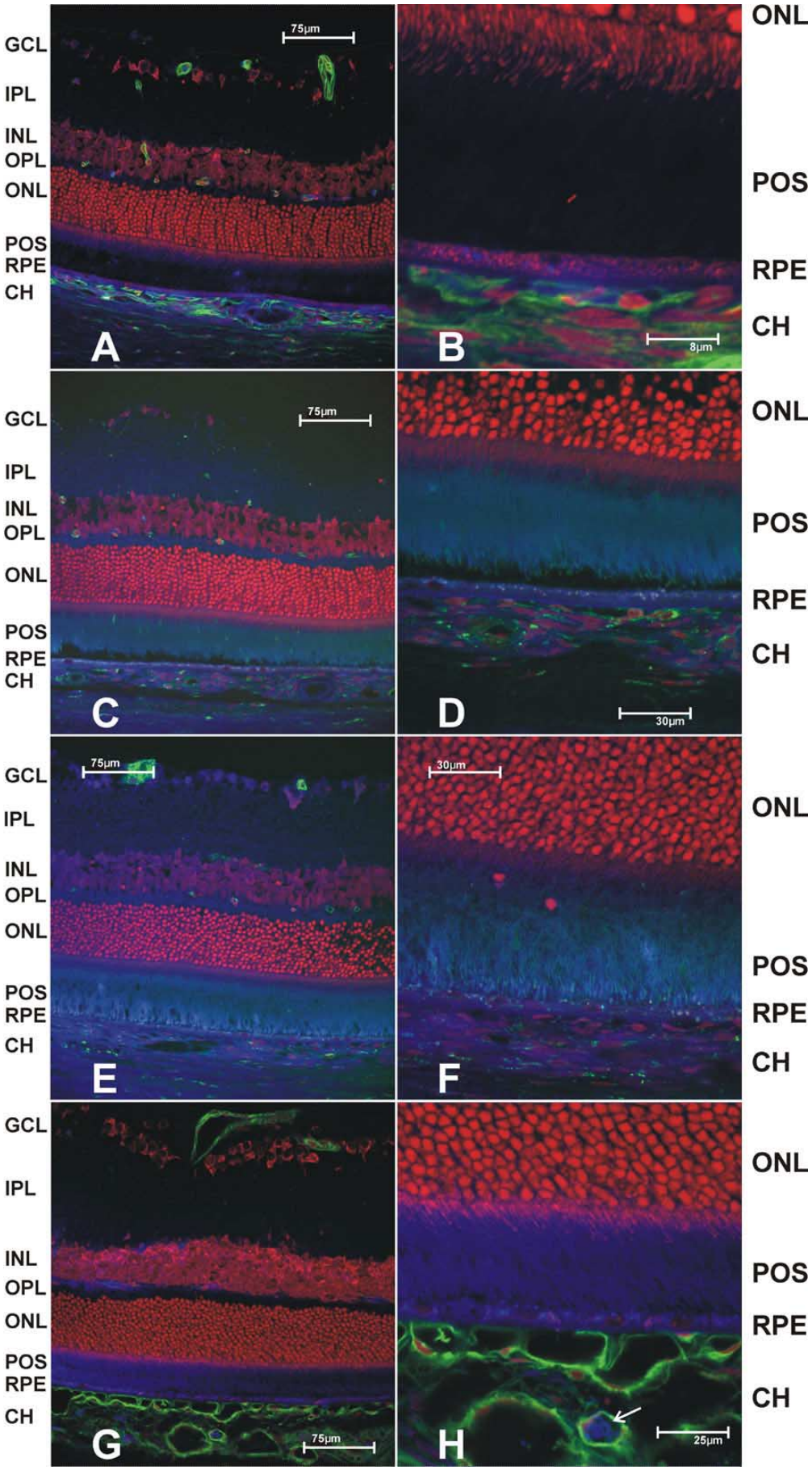

Figure 1. Cholestatrienol low density lipoprotein uptake by the rat retina. Vibrotome sections of rat retina imaged by confocal microscopy after intravenous injection with the fluorescent cholesterol analog cholestatrienol (CTL; blue) complexed with human low density lipoprotein (LDL). Rats were injected with 2 mg of cholestatrienol-low density lipoprotein (CTL-LDL) and sacrificed at different time intervals. The nuclei were stained with propidium iodide (red) and the capillaries were stained with Alexa 488®-conjugated isolectin IB4 (green). **A** and **B**: 2 h post-injection; **C** and **D**: 4 h post-injection; **E** and **F**: 6 h post-injection; **G** and **H**: 24 h post-injection. Arrow points to LDL deposit remaining in the choroid after 24 h.

retina: The levels of HDL in rat serum are approximately twice those of LDL (ca. 40 mg/dl HDL versus ca 20 mg/dl LDL) [26]. Hence, in addition to its established role in reverse cholesterol transport i.e., from the peripheral tissues back to the liver; reviewed in [27] it seems at least possible that HDL could also be a source of lipids to the retina. Therefore, CTL-HDL was prepared and injected intravenously into the rats (see Materials and Methods); CTL-LDL was also injected for direct comparison. The amount of CTL-LDL was the same as shown in Figure 1 (2 mg). The amount of CTL-HDL was approximately 1.5 mg, because the injected amounts were calculated based on the levels of CTL. HDL, perhaps due to its

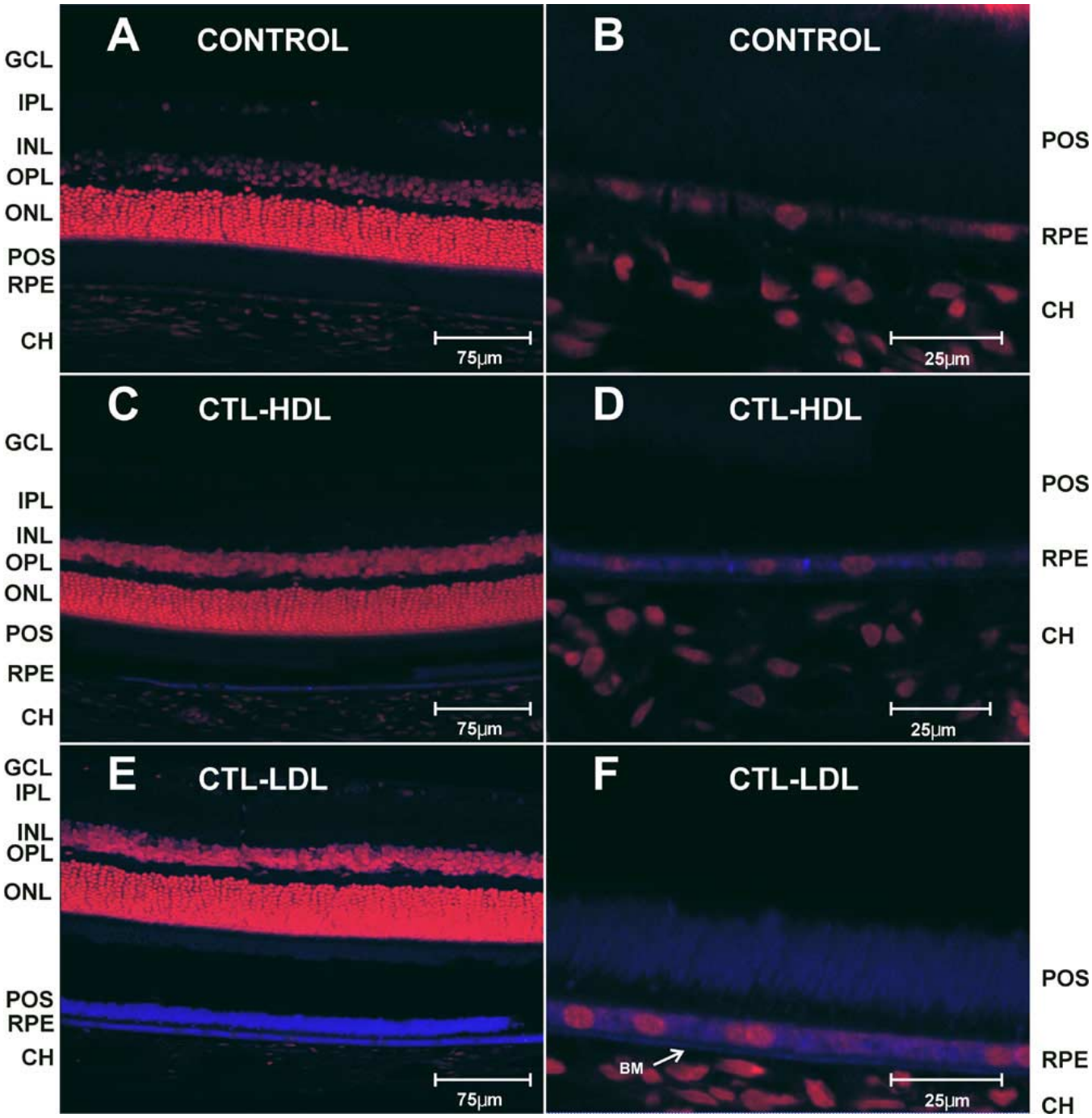

Figure 2. Comparison of cholestatrienol uptake by the rat retina via high density lipoprotein versus low density lipoprotein. Rats were injected intravenously with cholestatrienol-low density lipoprotein (CTL-LDL; 2 mg, blue) and cholestatrienol-high density lipoprotein (CTL-HDL; 1.5 mg, blue), then sacrificed 4 h post-injection (see Materials and Methods). Vibrotome sections were prepared and nuclei counter-stained with propidium iodide (red) before imaging by confocal microscopy. The retinas were imaged under identical conditions and at two different magnifications. **A** and **B** are control retinas from rats that received no injections. **C** and **D** are retinas from CTL-HDL injected rats. **E** and **F** are retinas from CTL-LDL injected rats.

smaller particle size and greater surface area compared to LDL, seems to take-up approximately 50% more CTL than does LDL. The rats were injected, then euthanized after 4 h and the CTL was imaged as described above. The CTL-HDL was observed mostly in the RPE, but at significantly lower levels than when CTL-LDL was employed (Figure 2). Thus, under the conditions used, LDL was more readily taken up by the RPE and retina than was HDL, suggesting that LDL is the dominant vehicle for delivery of blood-borne cholesterol to the RPE and neural retina.

Localization of human apoB in the rat retina 4 h after human low density lipoprotein injection: In order to determine if apoB from the intravenously supplied human LDL had been taken up by the retina, immunohistochemistry and

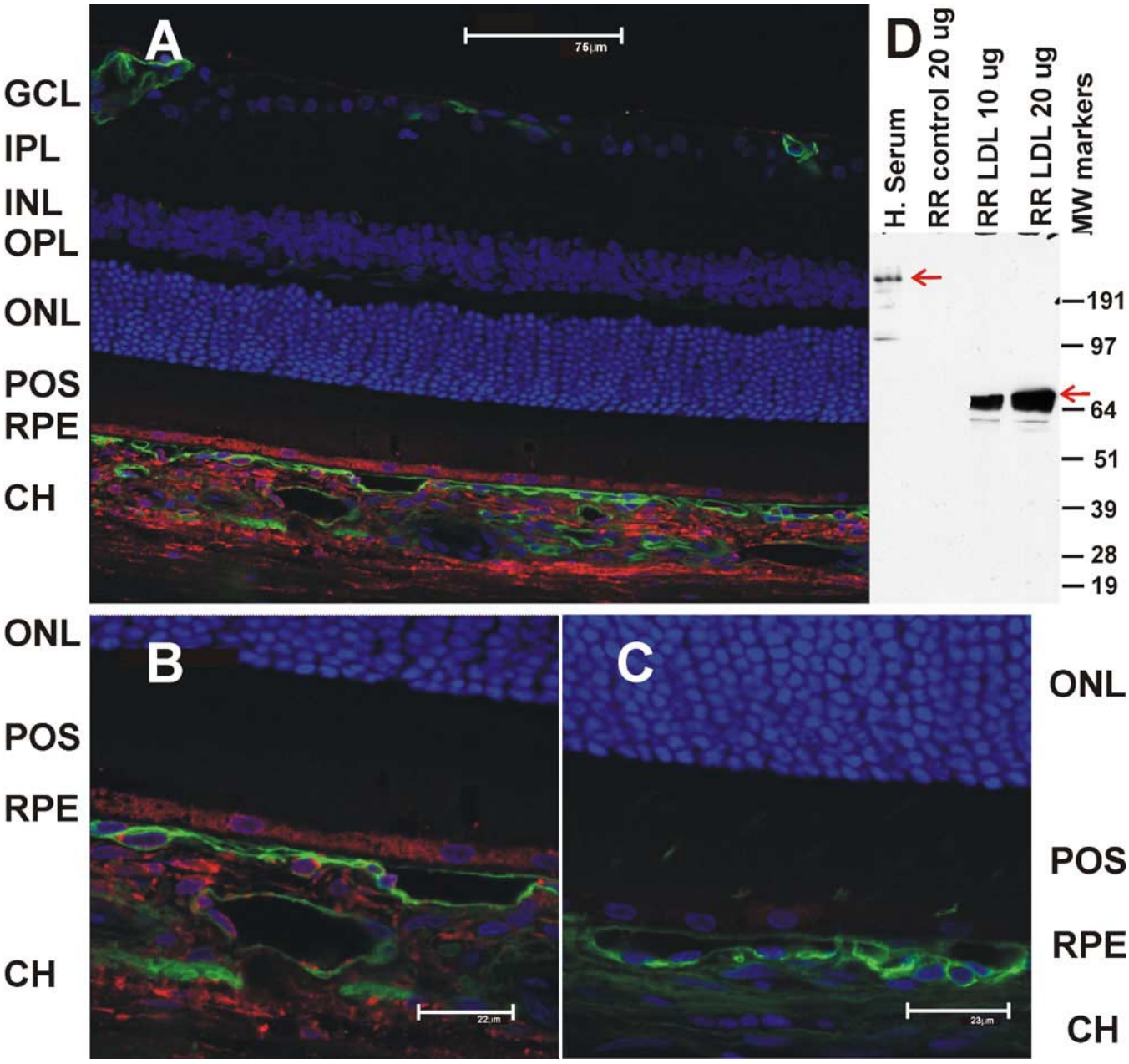

Figure 3. Immunohistochemical localization of human apoB in the rat retina 4 h after human low density lipoprotein injection. Vibrotome sections of rat retina 4 h post-injection with human CTL-LDL were imaged by confocal microscopy after incubation with anti-human apoB (1:200). The anti-human apoB immunoreactivity was detected using a Alexa Fluor® 633-conjugated donkey anti-sheep secondary antibody (red; see Materials and Methods). The nuclei were stained with DAPI (blue) and capillaries were stained with Alexa 488®-conjugated isolectin IB4 (green). **A**: Low magnification of the rat retina demonstrating human apoB immunoreactivity in the choriocapillaris (CH) and RPE. **B**: Higher magnification of the CH and RPE regions. **C**: Control retina (no LDL injection). **D**: Immunoblot of CTL-LDL injected and untreated rat retina (RR) demonstrating the 70 kDa (lower arrow) processed form of human apoB. Human serum was used a positive control for apoB (upper arrow).

Table 1. Total ion current measurements of cholesterol (Ch) and deuterated cholesterol (D7Ch) in rat retina and brain tissue

	Ch (m/z:369)	D7Ch (m/z 376)	Ch:D7Ch ratio
Rat retinas (12)	8103	220	38
Rat brain (6)	8272	12	690

These measurements are based on experiments like the one shown in Figure 3. In order to adequately quantify both ions, samples were run at three different concentrations. The cholesterol values were determined from the diluted injections to avoid detector "dead time". In case of the brain samples only the most concentrated (D7Ch) and most dilute (Ch) were useful for quantifications. In the pooled retina sample, the D7Ch value is an average of three measurements normalized for dilution. The Ch value is based on the average of the two measurements from the intermediate and highest dilutions.

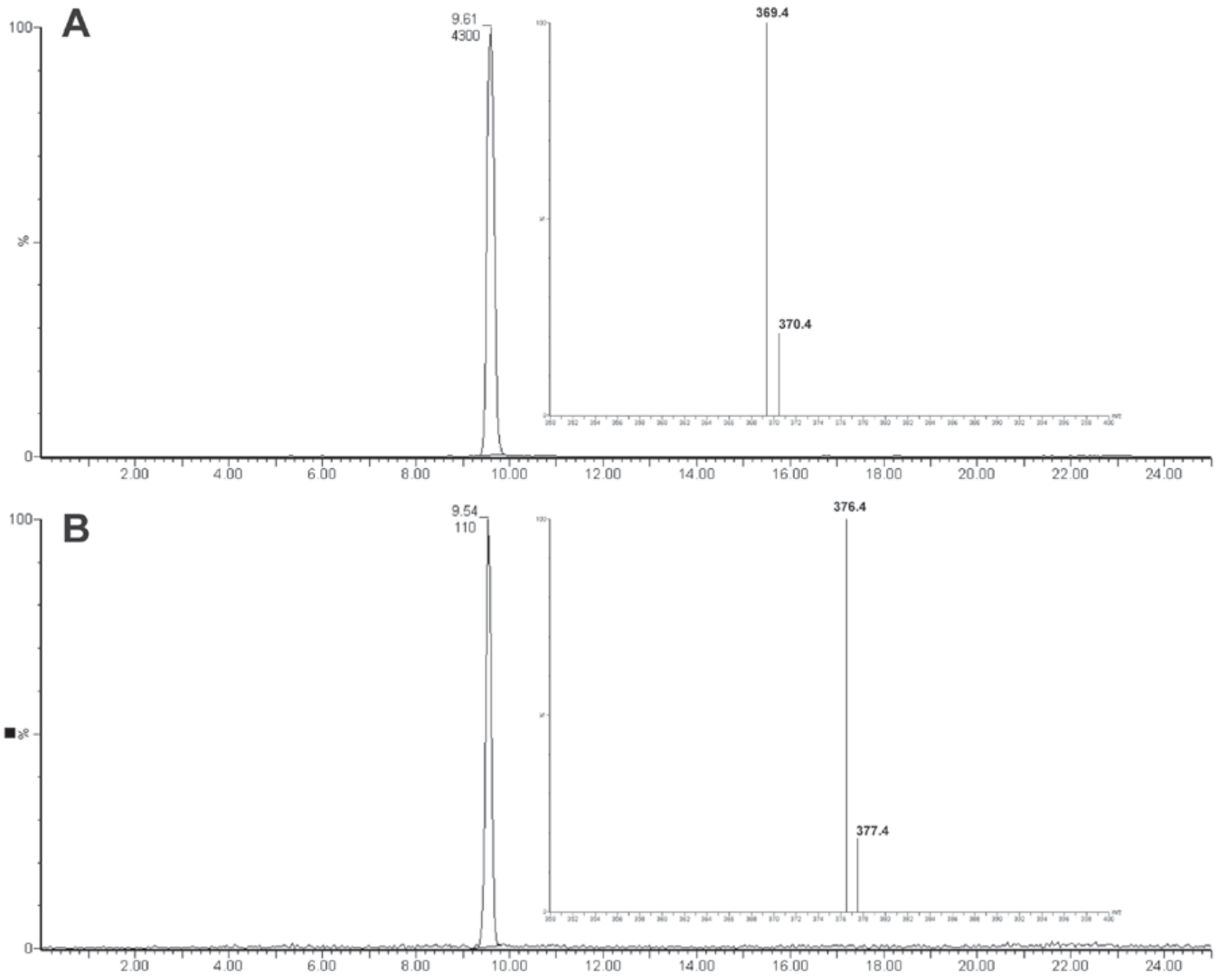

Figure 4. HPLC-MS analysis of saponified rat retina extracts 4 h after injection with deuterated cholesterol-low density lipoprotein. The chromatogram demonstrates the total ion current (TIC) for (**A**) the m/z 369 (cholesterol) and (**B**) the m/z 376 deuterated cholesterol (D7Ch). Insets show the spectrum of each ion. Quantification was performed by TIC peak area integration. In this particular example, analysis shows a 39:1 M ratio of cholesterol (Ch) to D7Ch. The average values obtained from three separate analyses at different concentrations are shown in Table 1.

immunoblot analyses were performed at 4 h post-injection using an antibody specific to human apoB, the major protein constituent of LDL. Rat retina vibrotome sections were prepared and immunostained (see Materials and Methods). Anti-human apoB IgG was detected using a red-fluorescing Alexa Fluor® 633-conjugated secondary antibody. Human apoB was detected mainly in the choriocapillaris and RPE (red fluorescence, Figure 3A,B). The anti-human apoB antibody employed exhibits no cross-reactivity with any other rat retina proteins, as shown by immunofluorescene of a control rat retina (from a rat not injected with LDL; Figure 3C) and in the companion immunoblot controls (Figure 3D). In retinas of LDL-injected rats, Western blot analysis showed a M_r. Around 70 kDa apoB-immunopositive band, suggesting that apoB was partially degraded [28]. By contrast, human serum (positive control) exhibited an immunoreactive band at M_r around 540 kDa presumably corresponding to native (full size) apoB (Figure 3D). This further demonstrates that the intravenously administered human LDL was able to enter the retina via the RPE-choriocapillaris route, whereupon it was partially metabolized. This is consistent with the results shown in Figure 1 and Figure 2.

Quantification of cholesterol uptake by the rat retina: For quantification of LDL-cholesterol mediated uptake by the retina, we replaced CTL with deuterated cholesterol (D7Ch). The use of D7Ch provides the advantage over CTL of greater stability during saponification and identical ionization condition to cholesterol during mass spectroscopy (I.R. Rodriguez, unpublished results).

Six rats were injected with human D7Ch-LDL. The retinas (pooled, N=12, around 1 mg wet wt. per retina) and a small portion of brain cortex were harvested 4 h post-injection, washed three times with PBS to remove any extraneous blood, then saponified and non-saponifiable lipids were extracted and analyzed by HPLC-MS (see Materials and Methods). Since the brain is known not to take up circulating cholesterol [19], the brain samples served as a "negative uptake control" for the retina. The results of this experiment are shown in Table 1. Cholesterol was identified by its retention time (9.60 min) and its mass-to-charge ratio (m/z 369 daltons). Cholesterol, when ionized under the conditions employed, generates a mass ion that results from the loss of the C-3β hydroxyl ion $(M\text{-}OH)^+$. The deuterated cholesterol (with 7 deuterium atoms per molecule) generates a m/z 376 ion. Quantification is performed by integrating the total ion current (TIC) for the respective ions, m/z 369 for cholesterol and m/z 376 for D7Ch. A representative chromatogram and corresponding spectra are shown in Figure 4. After 4 h the ratio of total cholesterol to newly internalized (exogenous) cholesterol is approximately 39:1. This means that approximately 2.5% of the total cholesterol in the rat retina can be replaced in 4 h by cholesterol from extra-retinal (blood-borne) sources.

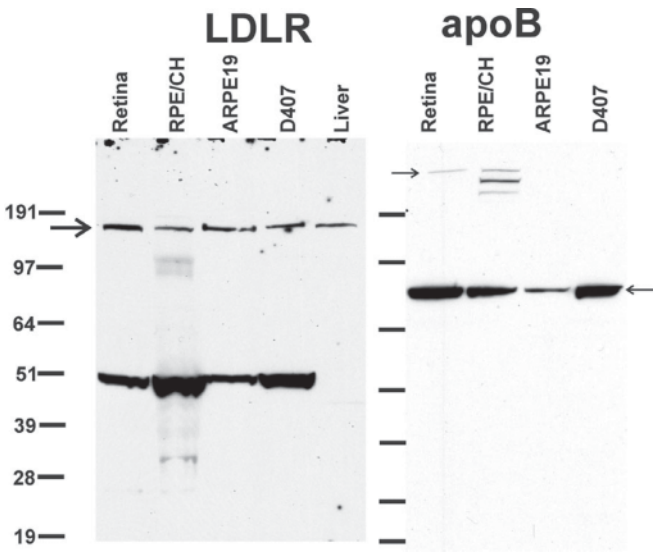

Figure 5. Immunoblots demonstrating LDLR and apoB expression. Expression of LDLR and apoB were determined by SDS-PAGE and the immunoblots for both antibodies were developed under identical conditions. SDS-PAGE and blots for both samples were run under identical conditions (see Materials and Methods). The right-pointing arrows mark expected molecular size for low density lipoprotein receptor (ca. 120 and 160 kDa) and apoB (ca. 540 kDa). The left-pointing arrow mark the apoB 70 kDa degradation product.

Expression of low density lipoprotein receptor and apoB in monkey retina: We extended these studies to the monkey retina for several reasons. First, from a practical standpoint, most of the commercially available antibodies to the known lipid transport proteins have been raised against human proteins, and those antibodies readily cross-react with monkey tissues, but not with rat tissues. In addition, we have access to fresh monkey tissue, which provides excellent morphology when vibrotome sectioning is employed. By contrast, this is difficult, if not impossible, to achieve with human postmortem tissue; previously published localizations of apoB in human retina clearly demonstrate this point [29]. Moreover, the primate eye replicates the essential anatomical features of the human eye, notably being the only other mammalian species that has a defined macula and fovea, with cone densities similar to those found in the human eye. Hence, findings obtained using monkey retinas are likely to provide insights directly relevant to lipid uptake processes in the human retina.

Immunoblots to detect LDLR and apoB were performed on monkey retina and on two human RPE-derived cell lines, ARPE19 and D407 (Figure 5). LDLR is generally detected as two bands (ca. 120 and 160 kDa), both of which were observed clearly in the neural retina sample. However, most of the immunoreactivity in all of the samples examined was observed in smaller-size bands, suggesting that LDLR is being rapidly processed in these tissues. This pattern of degradation was also observed in the two human RPE-derived cell lines, ARPE19 and D407. ApoB100 is readily detected in serum as a around 540 kDa protein; however, in our retinal samples, apoB was detected mainly as the proteolytically processed 70 kDa isoform [28]. The monkey neural retina and RPE-choroid fraction seem to contain only a very small amount of the full-size apoB (Figure 5, arrow), but this was not observed in immunoblots obtained using cultured RPE cells. This suggests that most of the apoB in the retina is in a state of being pro-

cessed and is like originates in the blood. The processed nature of both LDLR and apoB is consistent with the results obtained in the rat (Figure 3), which indicate a constant (constitutive, unregulated) uptake of circulating LDL by the retina (see Discussion).

Immunohistochemical localization of low density lipoprotein receptor in monkey retina: The retina is a complex organ system composed of at least 10 different types of cells [30,31], including six neuronal cell types. The organization of these cells is critical to the function of the retina. Thus, localization of proteins in the retina is particularly important to understanding their function.

Immunohistochemistry was performed on monkey retina vibrotome sections using antibodies to human LDLR (Figure 6). Immunoreactivity to LDLR was found in the ganglion cell layer (GCL), which includes Müller cell processes, and the outer plexiform layer (OPL) close to the area where photoreceptors and horizontal cells form their synapses (Figure 6A). The RPE and choriocapillaris (CH) also demonstrated a considerable amount of immunoreactivity (Figure 6C). In the RPE,

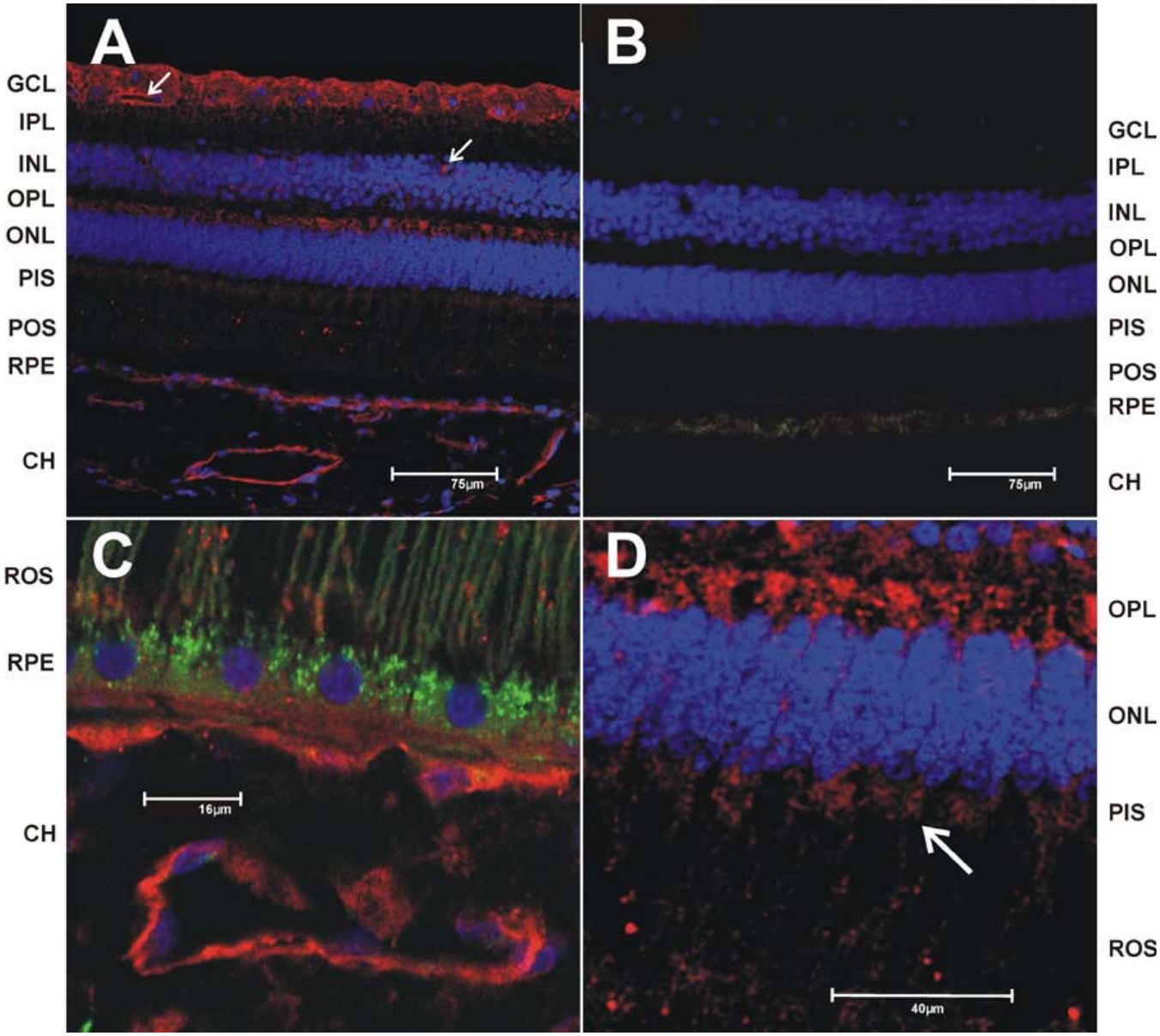

Figure 6. Immunohistochemical localization of low density lipoprotein receptor. Vibrotome sections of monkey retina were immunostained and imaged by confocal microscopy. The nuclei were stained with DAPI (blue), the primary antibodies was detected using Cy5-conjugated (red) secondary antibodies. **A**: low density lipoprotein receptor (LDLR) immunoreactivity detected with anti-human LDLR rabbit polyclonal antibody (Santa Cruz Biotechnology) at 1:100 dilution. The arrow points to a retinal capillary. **B**: Negative control (no primary antibody) at same magnification as (**A**). **C**: LDLR immunoreactivity at higher magnification focusing on the RPE/CH region. The green channel was added to allow visualization of the rod outer segments and the lipofuscin granules in the RPE by autofluorescence. **D**: Higher magnification of the photoreceptor inner segments and outer plexiform region (OPL).

LDLR immunoreactivity was decidedly polarized, being localized to the basal surface of the cells, which is the area exposed to the fenestrated choriocapillaris. The photoreceptor inner segments (cell bodies) were also faintly labeled (Figure 6D, see arrow). A negative control (no primary antibody) is shown in Figure 6B.

Immunohistochemical localization of apoB in monkey retina: ApoB immunostaining was not clearly detected in the inner retina except at the location of the retinal capillaries (Figure 7A, arrows). Most of the apoB immunoreactivity was detected in the choriocapillaris and the RPE (Figure 6C,D). In the choriocapillaris apoB was observed in deposits on the luminal aspect of the endothelial cells (see arrow). This is consistent with the LDL deposits observed in the rat choriocapillaris after CTL-LDL injection (Figure 1). In the RPE, apoB clusters were found superimposed with lipofuscin granules (Figure 7C). Labeling was also observed throughout Bruch's membrane. Faint immunostaining was observed in

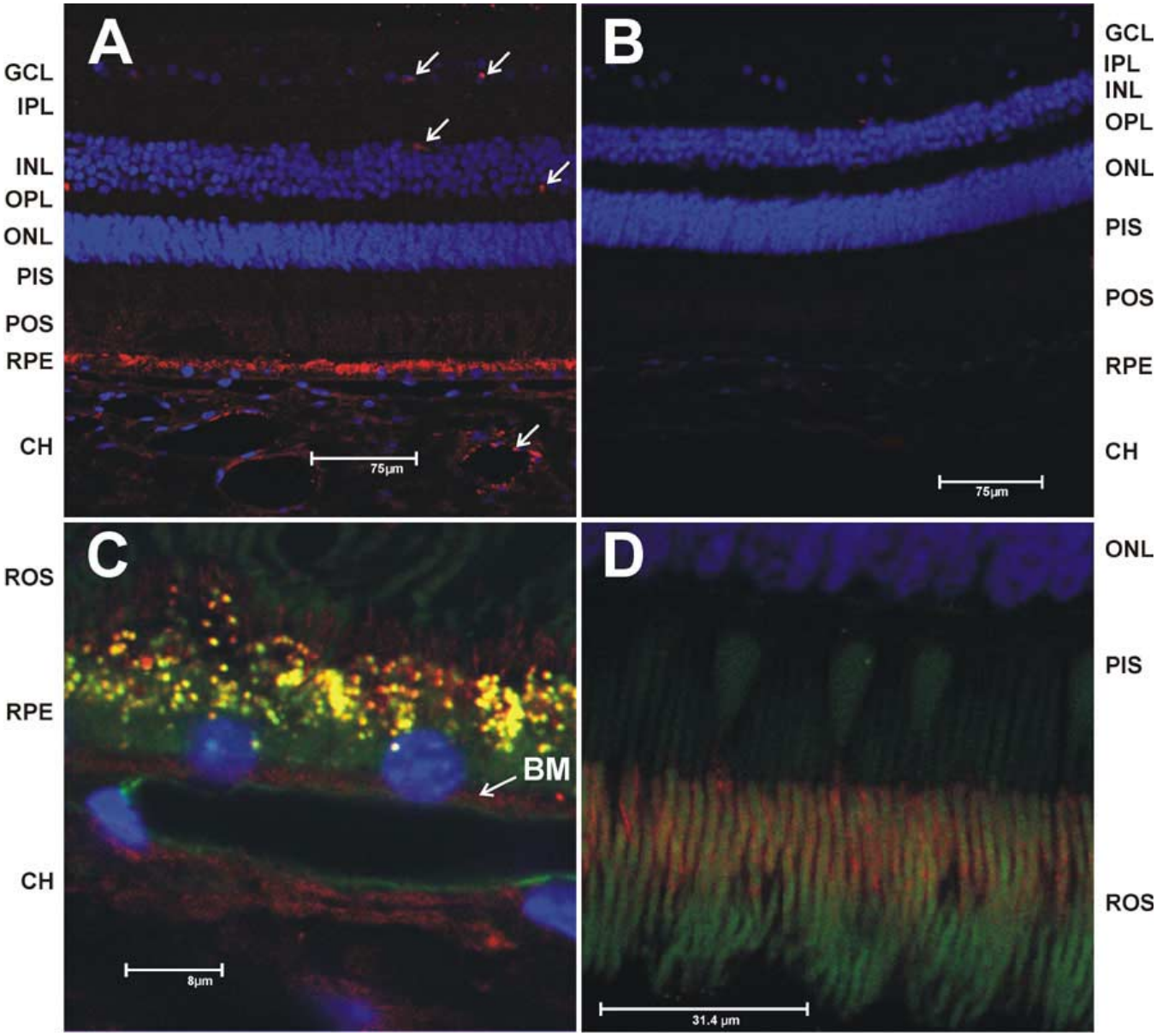

Figure 7. Immunohistochemical localization of apoB. The immunohistochemistry was performed as described in the Figure 6 legend (see also Materials and Methods). **A**: ApoB immunoreactivity detected with an anti-human apoB100 mouse monoclonal antibody (BD Biosciences) at 1:50 dilution. The top arrows point to immunoreactivity in retina capillaries. The lower arrow in the CH points to LDL deposits in the choroid. **B**: Negative control (no primary antibody) at same magnification as (**A**). **C**: ApoB immunoreactivity at higher magnification focusing on the RPE/CH region. The green channel was added to **C** and **D** to allow visualization by autofluorescence of the outer segments and lipofuscin deposits in the RPE. Yellow color in RPE demonstrates co-localization of the lipofuscin deposits (green) and the apoB immunoreactivity (red). The arrow points to punctate apoB immunoreactivity localized to Bruch's membrane (BM). **D**: Higher magnification of photoreceptor outer segment region with enhanced green channel autofuorecsence to demonstrate slight immunoreactivity in the IPM.

the photoreceptor outer segment layer (Figure 7D), possibly in the interphotoreceptor matrix (IPM). The possible presence of apoB in the IPM and LDLR in the photoreceptor inner segments and outer plexiform layer (OPL) suggests the presence of an endogenous LDL-like lipoprotein transport process. However, the overall localizations of apoB and LDLR and the results from the immunoblot analyses suggest uptake of exogenously supplied LDL particles is the dominant source of these particles in the retina. This is consistent with the results obtained using rats (Figure 1).

DISCUSSION

There is now considerable evidence demonstrating LDL uptake by the retina [8-13]. However, none of these previous reports used a cholesterol analog to demonstrate lipid uptake. Herein, we present the first such demonstration of exogenous sterol delivery to the retina using LDL modified with a cholesterol analog. We demonstrate that the fluorescent cholesterol analog, CTL, can be carried to the retina by exogenously administered human LDL in rats within 2 h of intravenous injection and can be observed in the photoreceptor outer segments by 4 h post-injection (Figure 1). CTL remained in the photoreceptor outer segments for at least 24 h (Figure 1). Since the RPE and neural retina normally contain no compounds having the fluorescence properties of CTL (see Figure 1A), and since CTL serves as an exceptionally reliable analog of cholesterol [21,24,25], these findings convincingly demonstrate that LDL-borne cholesterol can cross the blood-retina barrier and be taken up by and redistributed within the neural retina, including photoreceptor outer segments. Similar experiments done with CTL-HDL in direct comparison to CTL-LDL indicate that HDL may also serve as a source of lipids to the retina (Figure 2), albeit far less efficiently than LDL. These data strongly suggest that the cholesterol content of the retina is derived, in part, from an exogenous (extra-retinal) source, i.e., blood-borne lipoproteins. We also were able to detect immunoreactivity to human apoB in the choriocapillaris and RPE in rats injected with human LDL (Figure 3), thereby demonstrating uptake of circulating LDL particles by the RPE. Müller cells also may be involved in lipoprotein uptake, since we observed some faint diffuse apoB immunoreactivity around the retinal capillaries (Figure 3A and other sections not shown), consistent with Müller cell bodies.

Quantification of the LDL uptake by mass spectroscopy using deuterated cholesterol provides additional insight into cholesterol homeostasis in the retina (Table 1 and Figure 4). Under the given experimental conditions, we estimate that the rat retina can replace approximately 2.5% of its total cholesterol in 4 h using LDL as the cholesterol source. Thus, assuming a linear process, complete turnover of retinal cholesterol and replacement in total with exogenous cholesterol would take approximately 6-7 days under the conditions used. However, preliminary studies (S.J. Fliesler, unpublished results) employing [^{3}H]acetate-based metabolic labeling suggest that the in vivo half-time for turnover of *de novo* synthesized cholesterol in the rat retina is approximately 17.5 days, and that traces of de novo synthesized cholesterol persist in the retina for at least two months. In addition, the steady-state concentration of cholesterol in the rat retina can be altered by feeding rats a high-cholesterol diet (S.J. Fliesler, unpublished results). Hence, the exact dynamics of cholesterol turnover, including the relative contributions from endogenous (de novo) and exogenous (extra-retinal) sources, remain to be evaluated further. The fact that LDL also carries a significant amount of phospholipids, triglycerides and cholesteryl esters suggests that LDL also may represent a significant exogenous source of these other lipids in the retina, and affect their turnover. Moreover, considering that the rat is generally a nocturnal animal with low dietary lipid intake and low levels of blood cholesterol (male Sprague-Dawley rats 10-12 weeks, 75 mg/dl total cholesterol, taconic), this lipid turnover process may be considerably more robust in humans, which have greater metabolic demands on their visual system and have much greater levels of circulating cholesterol (200 mg/dl) [32]. Our results obtained with monkey retina with regard to LDLR and apoB expression and localization (Figure 5, Figure 6, and Figure 7) are consistent with rapid LDL internalization and processing.

Immunohistochemical staining in monkey retinas localized LDL receptor to the endothelial cells of the choriocapillaris, the basal RPE cell membrane, the photoreceptor inner segments, and the ganglion and Müller cells (Figure 6A,C). This suggests that LDLR-mediated LDL transport may be occurring from both exogenous (blood-borne) and endogenous (intra-retinal) sources. Endothelial cells of the choriocapillaris internalize LDL, as indicated directly from our study utilizing CTL-containing LDL (Figure 1). Whether the choroid is internalizing the circulating LDL for its own use or to somehow aid the RPE with its lipid transport is a question that needs to be further investigated. Two independent reports, based upon studies employing cultured RPE cells, suggest that LDLR expression is not well-regulated in the RPE [13,33], i.e., LDL uptake by RPE cells is a constitutive process. Cultured ARPE19 cells seem to be able to internalize large amounts of LDL and oxLDL [13,34]. In the liver, LDLR is known to be recycled [18], but a recycling mechanism in the RPE has not been demonstrated. The immunoblot in Figure 5 suggests that extensive processing and/or degradation of LDLR occurs in the monkey neural retina and RPE-choroid. Similar results were observed with the cultured RPE cell preparations (Figure 5). Hence, it is possible that, in the RPE-choroid and neural retina, LDLR recycling is limited by, and in competition with, the rate of receptor degradation. If true, this would imply that the dynamics of LDL/LDLR-mediated lipid transport in the RPE/retina are, in some respects, distinct from those operating in liver.

ApoB100 is a large (ca. 540 kDa) lipoprotein generally synthesized by the liver and serves as the protein backbone of the LDL particle [16,35]. In human retina apoB100 has been demonstrated to be expressed by the ganglion and RPE cells [29,36], suggesting that neural retina and RPE cells have the endogenous capacity to assemble LDL (or LDL-like) particles. In monkey retina, we observed apoB to be localized mainly to the RPE, Bruch's membrane, and the choroid (Figure 7A,C). In the neural retina apoB was found mainly associated with

the retinal capillaries and the Müller cells (Figure 7C) with very faint labeling in the photoreceptor outer segments (Figure 7D). In the RPE, apoB seems to be mostly complexed with the lipofuscin deposits (Figure 6D). This labeling pattern is consistent with the "clumps" of labeling observed in the RPE by Li et al. [29]. However, not all of the apoB immunoreactivity observed in the RPE co-localized with the lipofuscin granules (Figure 7C). The localization of apoB in the monkey retina also is consistent with the cellular localization of LDLR (Figure 6A,C). Under the conditions employed, immunoblots of monkey retina detected mostly the well-known 70 kDa apoB degradation product, which can be formed both by proteosomal and endoplasmic reticulum-mediated degradation processes [28]. A small amount of undegraded apoB was also detected (Figure 6). Hence, the retina may possess both endogenous and exogenously acquired apoB. Our data demonstrating uptake of exogenously administered LDL (Figure 1) and the immunohistochemical localization of LDLR (Figure 6A,C) clearly implicate an extra-retinal (blood-borne) source for the apoB found in the RPE/retina. The high level of the 70 kDa degradation product (Figure 5) and the co-localization of apoB with lipofuscin also support the notion that apoB arises in the retina from an exogenous source. However, the previously published data by other investigators [29,36] and our detection of a small amount of full-size (native) apoB in the neural retina (Figure 5) suggests that there may also be an endogenous source of apoB. The localization of LDLR in the rod inner segments and synapses (Figure 6D) and the localization of apoB in the Müller cells and photoreceptor outer segments (Figure 7D) strongly suggest that an LDL-like lipoprotein internal transport mechanism may be active in the retina.

The demonstration that LDL can quickly carry blood-borne cholesterol to the retina via an LDLR-mediate process raises a series of questions. How does cholesterol (and accompanying lipids) move from the suspected points of entry, the RPE and Müller cells, to the inner retina? Does the retina have the molecular mechanism for internal lipid transport? What is the nature of this transport mechanism? These questions are the focus of our companion paper (Tserentsoodol et al.) [37].

ACKNOWLEDGEMENTS

The authors would like to thank Dr. Richard C. Hunt for his kind gift of D407 cells. IRR was supported by the National Eye Institute intramural research program. SJF was supported, in part, by U.S.P.H.S. grant EY07361, by the Norman J. Stupp Foundation Charitable Trust, and by an unrestricted grant from Research to Prevent Blindness.

REFERENCES

1. Fliesler SJ, Florman R, Rapp LM, Pittler SJ, Keller RK. In vivo biosynthesis of cholesterol in the rat retina. FEBS Lett 1993; 335:234-8.
2. Bazan NG, Rodriguez de Turco EB. Review: pharmacological manipulation of docosahexaenoic-phospholipid biosynthesis in photoreceptor cells: implications in retinal degeneration. J Ocul Pharmacol 1994; 10:591-604.
3. Fliesler SJ, Keller RK. Isoprenoid metabolism in the vertebrate retina. Int J Biochem Cell Biol 1997; 29:877-94.
4. Giusto NM, Pasquare SJ, Salvador GA, Castagnet PI, Roque ME, Ilincheta de Boschero MG. Lipid metabolism in vertebrate retinal rod outer segments. Prog Lipid Res 2000; 39:315-91.
5. Caputto BL, Guido ME. Shedding light on the metabolism of phospholipids in the retina. Biochim Biophys Acta 2002; 1583:1-12.
6. Hayes KC, Lindsey S, Stephan ZF, Brecker D. Retinal pigment epithelium possesses both LDL and scavenger receptor activity. Invest Ophthalmol Vis Sci 1989; 30:225-32.
7. Duncan KG, Bailey KR, Kane JP, Schwartz DM. Human retinal pigment epithelial cells express scavenger receptors BI and BII. Biochem Biophys Res Commun 2002; 292:1017-22.
8. Bazan NG, Gordon WC, Rodriguez de Turco EB. Docosahexaenoic acid uptake and metabolism in photoreceptors: retinal conservation by an efficient retinal pigment epithelial cell-mediated recycling process. Adv Exp Med Biol 1992; 318:295-306.
9. Wang N, Anderson RE. Transport of 22:6n-3 in the plasma and uptake into retinal pigment epithelium and retina. Exp Eye Res 1993; 57:225-33.
10. Elner VM. Retinal pigment epithelial acid lipase activity and lipoprotein receptors: effects of dietary omega-3 fatty acids. Trans Am Ophthalmol Soc 2002; 100:301-38.
11. Miller JW, Walsh AW, Kramer M, Hasan T, Michaud N, Flotte TJ, Haimovici R, Gragoudas ES. Photodynamic therapy of experimental choroidal neovascularization using lipoprotein-delivered benzoporphyrin. Arch Ophthalmol 1995; 113:810-8.
12. Haimovici R, Kramer M, Miller JW, Hasan T, Flotte TJ, Schomacker KT, Gragoudas ES. Localization of lipoprotein-delivered benzoporphyrin derivative in the rabbit eye. Curr Eye Res 1997; 16:83-90.
13. Gordiyenko N, Campos M, Lee JW, Fariss RN, Sztein J, Rodriguez IR. RPE cells internalize low-density lipoprotein (LDL) and oxidized LDL (oxLDL) in large quantities in vitro and in vivo. Invest Ophthalmol Vis Sci 2004; 45:2822-9.
14. Wise GN, Dollery CT, Henkind P. The retinal circulation. New York: Harper and Row; 1971.
15. Guyer DR, Schachat AP, Green WR. The choroid: structural considerations. In: Ryan SJ, editor. Retina. 3rd ed. Vol 1. St. Louis: Mosby; 2001. p. 21-31.
16. Hevonoja T, Pentikainen MO, Hyvonen MT, Kovanen PT, Ala-Korpela M. Structure of low density lipoprotein (LDL) particles: basis for understanding molecular changes in modified LDL. Biochim Biophys Acta 2000; 1488:189-210.
17. Brown MS, Kovanen PT, Goldstein JL. Regulation of plasma cholesterol by lipoprotein receptors. Science 1981; 212:628-35.
18. Jeon H, Blacklow SC. Structure and physiologic function of the low-density lipoprotein receptor. Annu Rev Biochem 2005; 74:535-62.
19. Dietschy JM, Turley SD. Thematic review series: brain Lipids. Cholesterol metabolism in the central nervous system during early development and in the mature animal. J Lipid Res 2004; 45:1375-97.
20. Vance JE, Hayashi H, Karten B. Cholesterol homeostasis in neurons and glial cells. Semin Cell Dev Biol 2005; 16:193-212.
21. Fischer RT, Stephenson FA, Shafiee A, Schroeder F. delta 5,7,9(11)-Cholestatrien-3 beta-ol: a fluorescent cholesterol analogue. Chem Phys Lipids 1984; 36:1-14.
22. Rodriguez IR. Rapid analysis of oxysterols by HPLC and UV spectroscopy. Biotechniques 2004; 36:952-4,956,958.
23. HAVEL RJ, EDER HA, BRAGDON JH. The distribution and chemical composition of ultracentrifugally separated lipoproteins in human serum. J Clin Invest 1955; 34:1345-53.

24. Scheidt HA, Muller P, Herrmann A, Huster D. The potential of fluorescent and spin-labeled steroid analogs to mimic natural cholesterol. J Biol Chem 2003; 278:45563-9.
25. Bjorkqvist YJ, Nyholm TK, Slotte JP, Ramstedt B. Domain formation and stability in complex lipid bilayers as reported by cholestatrienol. Biophys J 2005; 88:4054-63.
26. Ness GC, Lopez D, Chambers CM, Newsome WP, Cornelius P, Long CA, Harwood HJ Jr. Effects of L-triiodothyronine and the thyromimetic L-94901 on serum lipoprotein levels and hepatic low-density lipoprotein receptor, 3-hydroxy-3-methylglutaryl coenzyme A reductase, and apo A-I gene expression. Biochem Pharmacol 1998; 56:121-9.
27. Lewis GF, Rader DJ. New insights into the regulation of HDL metabolism and reverse cholesterol transport. Circ Res 2005; 96:1221-32.
28. Cavallo D, Rudy D, Mohammadi A, Macri J, Adeli K. Studies on degradative mechanisms mediating post-translational fragmentation of apolipoprotein B and the generation of the 70-kDa fragment. J Biol Chem 1999; 274:23135-43.
29. Li CM, Presley JB, Zhang X, Dashti N, Chung BH, Medeiros NE, Guidry C, Curcio CA. Retina expresses microsomal triglyceride transfer protein: implications for age-related maculopathy. J Lipid Res 2005; 46:628-40.
30. Rodieck RW. The vertebrate retina: principles of structure and function. San Francisco: Freeman; 1973.
31. Kolb H. The neural organization of the human retina. In: Heckenlively JR, Arden GB, editors. Principles and practices of clinical electrophysiology of vision. St. Louis: Mosby; 1991. p. 25-52.
32. Sacks FM, Pfeffer MA, Moye LA, Rouleau JL, Rutherford JD, Cole TG, Brown L, Warnica JW, Arnold JM, Wun CC, Davis BR, Braunwald E. The effect of pravastatin on coronary events after myocardial infarction in patients with average cholesterol levels. Cholesterol and Recurrent Events Trial investigators. N Engl J Med 1996; 335:1001-9.
33. Noske UM, Schmidt-Erfurth U, Meyer C, Diddens H. [Lipid metabolism in retinal pigment epithelium. Possible significance of lipoprotein receptors]. Ophthalmologe 1998; 95:814-9.
34. Rodriguez IR, Alam S, Lee JW. Cytotoxicity of oxidized low-density lipoprotein in cultured RPE cells is dependent on the formation of 7-ketocholesterol. Invest Ophthalmol Vis Sci 2004; 45:2830-7.
35. Schumaker VN, Phillips ML, Chatterton JE. Apolipoprotein B and low-density lipoprotein structure: implications for biosynthesis of triglyceride-rich lipoproteins. Adv Protein Chem 1994; 45:205-48.
36. Malek G, Li CM, Guidry C, Medeiros NE, Curcio CA. Apolipoprotein B in cholesterol-containing drusen and basal deposits of human eyes with age-related maculopathy. Am J Pathol 2003; 162:413-25.
37. Tserentsoodol N, Gordiyenko NV, Pascual I, Lee JW, Fliesler SJ, Rodriguez IR. Intraretinal lipid transport is dependent on high density lipoprotein-like particles and class B scavenger receptors. Mol Vis 2006; 12:1319-33.

The print version of this article was created on 27 Oct 2006. This reflects all typographical corrections and errata to the article through that date. Details of any changes may be found in the online version of the article.